

# **A PHENOMENOLOGICAL NUMERICAL MODEL FOR FUSED DEPOSITION PROCESSING OF PARTICLE FILLED PARTS**

M. Atif Yardımcı      Selçuk I Güçeri  
Mechanical Engineering Department  
University of Illinois at Chicago

Stephen C. Danforth  
Ceramics Engineering Department  
Rutgers University

## **ABSTRACT**

Fused Deposition Modeling<sup>TM</sup> utilizes the simple idea of melting, extrusion and resolidification of thermoplastic filaments. The introduction of particulate materials, especially ceramics and metals, will widen the range of capabilities of the process. The present study is directed to the development of a family of numerical models for the FDM and Fused Deposition of Ceramics processes. These models in turn would help to predict the operation windows of the FDM/FDC. Time-dependent mesh generation and parameter file generation are incorporated into the developed two-dimensional model. Finite element method is used in order to address heat transfer issues regarding the solidification of the thermoplastic binder.

## **INTRODUCTION**

FDM is a relatively young solid freeform fabrication technology (Crump,1992); and it has been commercialized and has been applied to a number of thermoplastic materials (Comb et.al, 1994). Fused Deposition of Ceramics is a new technology based on the development of the FDM hardware/knowledge base (Agarwala,1995). The current modeling study is part of this development effort. There are numerical modeling studies available in literature on stereolithography [(Flach and Chartoff, 1994), (Chambers et.al, 1994), (Wiedemann et.al., 1995)], and on selective laser sintering (Nelson et.al, 1993). Although FDM/FDC share a number of process characteristics with laser-based methods, the basic unit of production is fundamentally different. Hence different modeling approaches were required by the process.

The operation sequence in FDM/FDC may be thought as nested loops of the same unit operations; and the basic unit operation is the forming of a finite length road on the deposition table. This unit process has two distinct phases: i).the sequence of partial melting, extrusion, road initiation and ii) road consolidation and cooling. First phase

occurs in the near vicinity of the extrusion head, multi-phase flows and heat transfer are the relevant physical processes involved. Second phase, on the other hand, happens in the bulk of the body as newly formed interacts with the bulk of material thermally; conduction heat transfer with phase change is the main mode of the energy transfer. There is very limited relative motion, in contrast to the first phase.

Clearly different modeling approaches are needed for each phase of the process. In this work, a family of tools are developed for the second phase of the unit process. These include a one-dimensional analytical model, a one-dimensional numerical model including phase change and a two-dimensional numerical thermal model. Finite element method was used in the numerical models to solve the enthalpy form of the energy equation. The ability of models to simulate road cooling and consolidation has been demonstrated by exemplary test cases.

## ONE DIMENSIONAL MODELS

The roads produced have rectangular cross-sections The three dimensional heat transfer equation may be integrated along the coordinates axes aligned with the height and the width of the road. Assuming that the road is being formed on an adiabatic surface and neglecting the heat loss from the tip of the road we may idealize the road into a continuously elongating line. The governing equation for this idealized model is:

$$\frac{\partial T}{\partial t} = \frac{k}{\rho C_p} \frac{\partial^2 T}{\partial x^2} - \frac{h}{\rho C_p} \left( \frac{1}{height} + \frac{2}{width} \right) (T - T_\infty) \quad (1.a)$$

,with the boundary and initial conditions

$$@ t=0 \quad x \in [0, \varepsilon] \quad , \quad T = T_0 \quad (1.b)$$

$$@ \quad x=0 \quad , \quad \frac{\partial T}{\partial x} = 0 \quad (1.c)$$

$$@ \quad x = u * t \quad , \quad T = T_0 \quad (1.d)$$

It is obvious that, Equation (1.a) has been written for a reference frame attached to the deposition table. On the other hand; if we fix our reference frame to the extrusion head, time-dependence in the governing equation will drop out. Furthermore by simplifying the tip boundary condition we obtain a much simpler boundary value problem for an ODE:

$$\frac{dT}{dx} = \frac{k}{\rho C_p u} \frac{d^2 T}{dx^2} - \frac{h}{\rho C_p u} \left( \frac{1}{height} + \frac{2}{width} \right) (T - T_\infty) \quad (2.a)$$

, with

$$@ x \rightarrow \infty \quad , \quad T = T_\infty \quad (2.b)$$

$$@ x = 0 \quad , \quad T = T_0 \quad (2.c)$$

Equations 2.a, 2.b, 2.c. have a solution of form

$$T(x) = (T_0 - T_\infty)e^{-rx} + T_\infty \quad (3)$$

; with 
$$r = \frac{\sqrt{\beta_1^2 + 4\beta_2} - \beta_1}{2},$$

$$\beta_1 = \frac{\rho C_p u}{k}, \quad \beta_2 = \frac{h}{k} \left( \frac{1}{\text{height}} + \frac{2}{\text{width}} \right)$$

If a "cure" temperature,  $T_s$ , can be defined for the given material, below which diffusive bonding would be ineffective; then we could solve equation (3) for the active length of the road. Thus,

$$x_s = -\frac{\ln\left(\frac{T_s - T_\infty}{T_0 - T_\infty}\right)}{r} \quad (4)$$

Since  $r$  involves process parameters,  $x_s$  will be function of them. Grouping process parameters into doublets, calculating and drawing  $x_s$  surfaces process windows can be constructed. One such surface is given in Figure 1, depicting the effect of variations in heat transfer coefficient and speed on the active road length. A contour of  $x=0.1\text{m}$  is also shown for representing a characteristic vector length. Thus for the given material the triangular region at the lower-right corner will produce high cooling and improper bonding.

There are basically two ways by which phase change could be incorporated into the existing model. Enthalpy method was chosen to implement phase change. Thus the governing equation becomes:

$$\rho u \frac{d\hat{h}}{dx} = k \frac{d^2 T}{dx^2} - h \left( \frac{1}{\text{height}} + \frac{2}{\text{width}} \right) (T - T_\infty) \quad (5)$$

together with boundary conditions (2.b),(2.c) and the enthalpy - temperature relationships

$$\hat{h} = \int_{T_\infty}^T C_p(T) dT = f(T) \quad \text{and} \quad T = g(\hat{h}) \quad (6)$$

These system of equations are solved with one-dimensional finite-elements. The model was run for RU160 material, to observe the effect of process parameters on temperature distribution. The effect of road formation speed on temperature distribution is presented in Figure 2. Although the specific heat signature of RU160 does have a local maximum in the studied temperature range; The standard deviation is about 10% in the temperature interval investigated. Thus an effective specific heat may be defined for RU160 for this temperature range, and the fast one-dimensional analytical model may be utilized as a prediction tool.

## TWO DIMENSIONAL MODEL

Although one dimensional models are capable of modeling a single filament, multi-dimensional models are needed to capture the physics of road-road and road-slice interactions. In the presence of a neighboring road, the symmetry in temperature distribution is broken down. Also the moving reference frame would complicate model formulation, due to the already intrinsic unsteadiness of build-up process. Hence, the coordinate system is fixed with the table.

Again we will be focusing on roads being formed on an adiabatic foundation. Integrating the three-dimensional version of the energy equation in enthalpy form along the height of the road we obtain:

$$\rho u \frac{\partial \hat{h}}{\partial t} = k \left[ \frac{\partial^2 T}{\partial x^2} + \frac{\partial^2 T}{\partial y^2} \right] - h \left( \frac{1}{\text{height}} \right) (T - T_\infty) \quad (7.a)$$

$$@ x=0 \quad , \quad -k \frac{\partial T}{\partial x} = h(T - T_\infty) \quad (7.b)$$

$$@ x = u * t \quad , \quad T = T_0 \quad (7.c)$$

$$@ y=0 \quad , \quad -k \frac{\partial T}{\partial y} = h(T - T_\infty) \quad (7.d)$$

$$@ y = \text{width} \quad , \quad k \frac{\partial T}{\partial y} = h(T - T_\infty) \quad (7.e)$$

$$@ t=0 \quad x \in [0, \varepsilon] \quad , \quad y \in [0, \text{width}] \quad , \quad T = T_0 \quad (7.f)$$

with the enthalpy-temperature relations of Equations (6)

Triangular finite elements with linear interpolation functions were utilized for the implicit Galerkin discretization of governing equation. The boundary condition (7.c) tells us that we need to update the solution domain continuously. Most of the algorithmic machinery in the code was written for the moving boundary condition, subsequent mesh generation and data handling.

A preliminary result for the lay-down of a single road is presented on Figure 3. This test case was for a material possessing well defined solidification range and latent heat. Other properties were selected similar to RU160 properties. The road length is 100 mm. The temperature distribution is shown in consecutive times. After the road was fully formed, simulation was continued to proceed two more seconds for the cool-down. This example demonstrates models ability to handle *move* and *delay* sequences.

## CONCLUSION

Three distinct models have been developed for FDM/FDC. One-dimensional analytical model is fast enough to become part of a feedback control loop and may be utilized with the use effective specific heat constants obtained from MDSC measurements. One dimensional numerical model may be utilized for different materials possessing more variable specific heat dependencies on temperature. Two dimensional model is utilized to model the road cooling of a single road with a move and delay scenario.

## ACKNOWLEDGMENT

The authors would like to thank to other members of SFF/FDC project for supplying RU160 specimens and their help. The authors gratefully acknowledge the support of this research by Advanced Research Projects Agency and Office of Naval Research, through grant ONR Contract No. N300014-94-C-0015.

## REFERENCES

1. Agarwala, M., 1995, "Fused Deposition of Ceramics," 1995 Annual Meeting of American Ceramics Society, May 1995, Cincinnati, OH.
2. Chambers R.S., Guess T.R. and Hinnerichs T.D, 1995, "A Phenomenological Finite Element Model of Part Building in the Stereolithography Process," Proceedings of the Sixth International Conference on Rapid Prototyping, University of Dayton, Dayton, Ohio, June 4-7 1995.
3. Comb, J., Priedemann, W. and Turley P., 1994, "Control Parameters and Material Selection Criteria for Fused Deposition Modeling", Proceedings of The 5th International Conference On Rapid Prototyping, University of Dayton
4. Crump, S.S., 1992, "Rapid Prototyping Using FDM<sup>TM</sup>: A Fast, Precise, Safe Technology", Proceedings of Solid Freeform Fabrication Symposium 1992, ed H.L Marcus et.al., University of Texas at Austin
5. Flach, L., Chartoff R., 1994, "Stereolithography Process Modeling: Shrinkage Prediction" Proceedings of The 5th International Conference On Rapid Prototyping, University of Dayton
6. Nelson, J.C., Xue, S., Barlow, J.W., Beaman, J.J., Marcus, H.L. and Bourell, D.L., 1993, "Model of the Selective Laser Sintering of Bisphenol-A Polycarbonate", Industrial and Engineering Chemistry, vol. 32, pp 2305-2317
7. Wiedemann, B., Dusel, K.H. and Eschl J., 1995, "Influence of the Polymerization Dynamics of Stereolithography Resins on Accuracy," Proceedings of the Sixth International Conference on Rapid Prototyping, University of Dayton, Dayton, Ohio, June 4-7 1995.

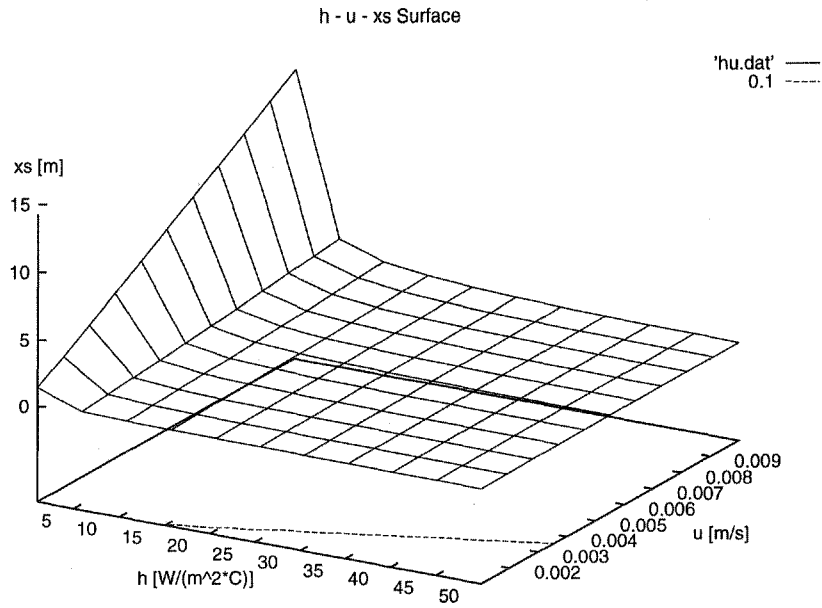


Figure 1. Operation window for RU160 like constant property material, with the properties:  $\rho=1700 \text{ kg/m}^3$ ,  $k=9 \text{ W/(m}^*\text{C)}$ ,  $C_p=2200 \text{ W/(m}^2*\text{C)}$ ,  $T_s=70\text{C}$ ; and process parameters :  $T_0=87.5 \text{ C}$ ,  $T_\infty=52.5 \text{ C}$ , height=0.55 mm, width=5\*height

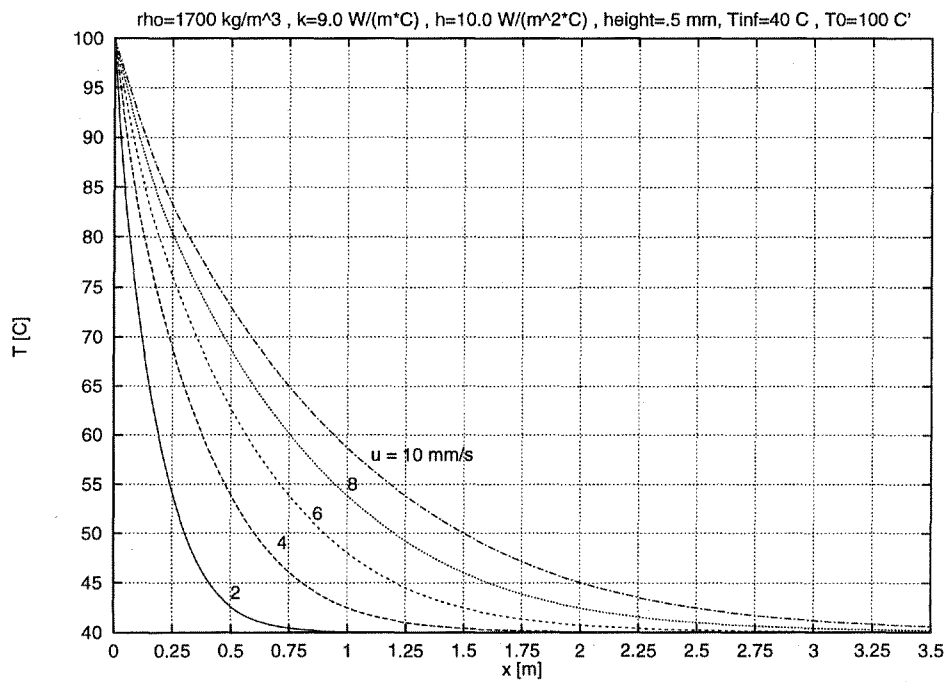


Figure 2. Effect of Speed Variation on Temperature Distribution

60% Filled Filament, Enthalpy Method  
 V= 10 mm/sec, Road Width = 1 mm, Road Height = 0.2 mm  
 Latent Heat of Solidification = 30 kJ/kg  
 Solidification Range = 45 - 55 C  
 Cp, density, k obtained by mixing rule and are constant.

195

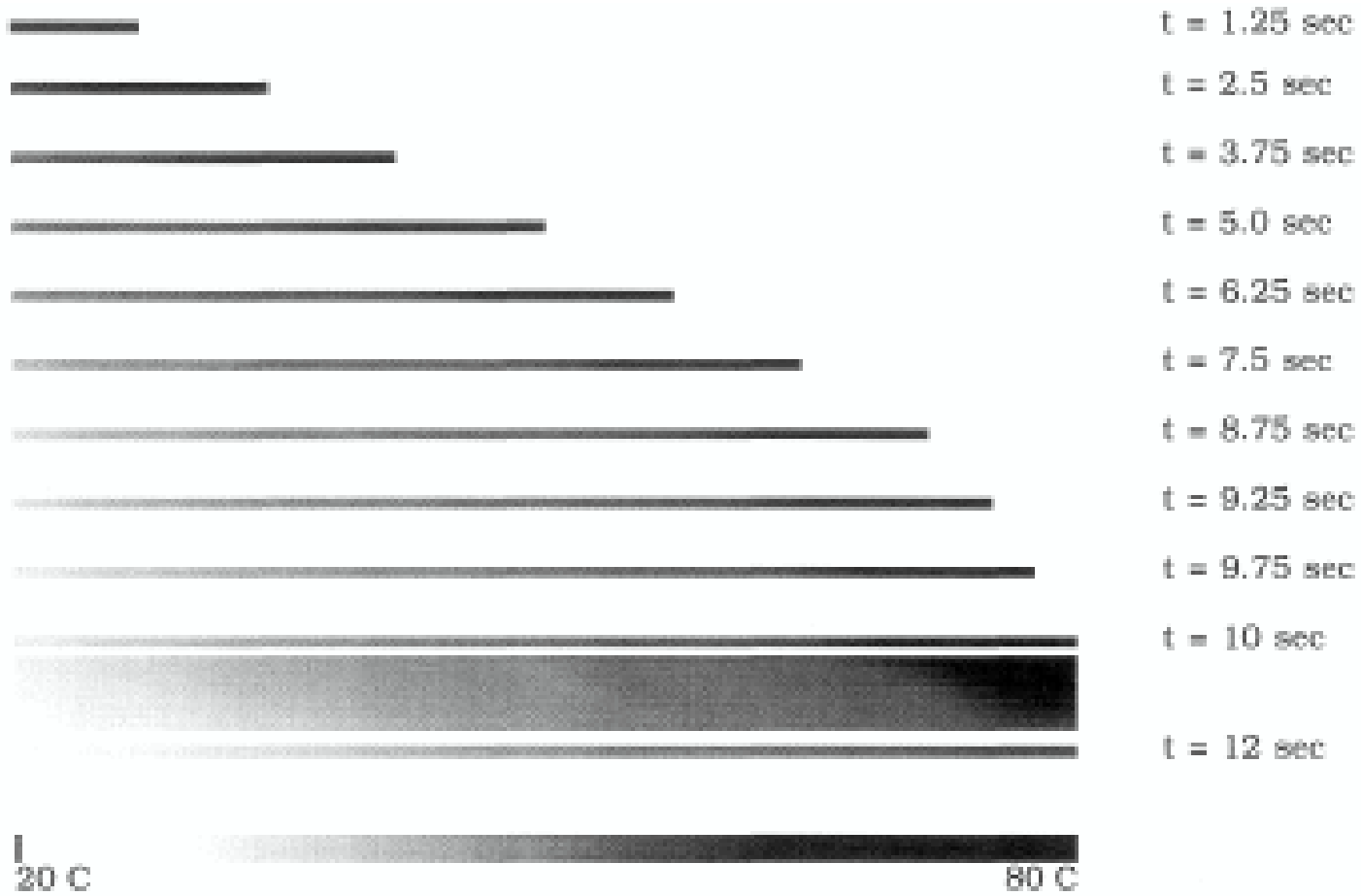


Figure 3. Road Cooling with Two Dimensional Model